Transient Shear Flow of a Unidomain Liquid Crystalline Polymer

I-Kuan Yang† and Annette D. Shine*

Department of Chemical Engineering, University of Delaware, Newark, Delaware 19716

Received September 9, 1992; Revised Manuscript Received December 3, 1992

ABSTRACT: The transient shear stress response of a unidomain liquid crystalline polymer has been analyzed using a two-dimensional approximation of the linear theory of Ericksen, Leslie, and Parodi. Under constant shear rate deformation, polymers with a negative Leslie coefficient α_3, which adopt a stable steady-state flow alignment angle, are predicted to exhibit a single stress maximum at a strain less than unity, while a tumbling nematic with $\alpha_3 > 0$ is predicted to exhibit the initial stress maximum at a strain greater than unity. The Leslie coefficients α_1, α_2, and α_3, as well as the Miesowicz viscosities η_c and η_b, were estimated from shear startup experiments for a unidomain solution of poly(*n*-hexyl isocyanate) (PHIC) in *p*-xylene and were compared with predictions from Doi's molecular theory of liquid crystalline polymers. The application of a transverse electric field to a tumbling nematic liquid crystalline polymer with positive dielectric anisotropy is predicted to cause the stress overshoot to occur at progressively smaller strain as the strength of the electric field is increased. At the critical field strength where tumbling is suppressed, the overshoot occurs at a strain near unity. Experiments with PHIC exhibit the predicted trends.

Introduction

The rheology of liquid crystalline polymers (LCPs) includes such unusual behavior as negative first normal stress differences,[1-4] very long relaxation times,[4] and oscillatory transient response to shear.[4-6] Currently, the most developed quantitative models of LCP rheology are the phenomenological theory of Ericksen, Leslie, and Parodi (ELP)[7-9] and the molecular theory of Hess,[10,11] as developed by Doi[12] for LCPs. Both theories are based on the assumption that the initial orientation of the LCP is spatially uniform, despite experimental evidence for a polydomain structure of LCPs. Nevertheless, versions of these two "unidomain" theories are frequently invoked to interpret the behavior of polydomain systems; qualitatively, the theories have succeeded to some extent in negative normal stress[13] and transient shear behavior.[5,14] However, the role of domain structure in LCP rheology has not been clearly identified, largely because the domain structure is poorly understood and thus difficult to control experimentally.

Rheological studies on unidomain LCPs could provide a direct test of the validity of unidomain theories. Optical studies of unidomain LCPs undergoing shear have been conducted on solutions of poly(benzobisthiazole)[15] and poly(benzyl L-glutamate)[16] and indicate that these LCPs exhibit director tumbling during shear flow. According to ELP theory, director tumbling occurs when the Leslie coefficient α_3 is positive, while a stable flow alignment of the director occurs when α_3 is negative. Unfortunately, the dynamic light scattering technique which has been used to determine the Leslie coefficients of LCPs is unable to distinguish the sign of α_3 due to the quadratic nature of the governing equations.[17,18] In this paper, we demonstrate theoretically how the sign of α_3 can be inferred from rheological measurements of a unidomain LCP, and we employ the theoretical analysis to derive experimental estimates for the Leslie coefficients for a unidomain solution of poly(*n*-hexyl isocyanate) in *p*-xylene. The unidomain texture is provided experimentally by application of an electric field before shearing is started. A comparison is made between the transient behavior of unidomain and polydomain solutions. Concurrent application of a transverse electric field during shear startup is also examined theoretically and experimentally.

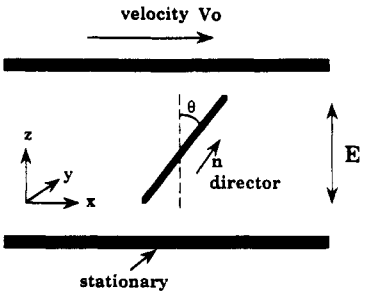

Figure 1. Coordinate system for 2-D analysis.

Theory

In this treatment, we adopt the two-dimensional approximation of ELP theory used by Carlsson and Skarp;[19] the coordinate system is shown in Figure 1. The xz component of the stress is given by

$$\tau = g(\theta)\frac{\partial v}{\partial z} + (\alpha_2 \cos^2\theta - \alpha_3 \sin^2\theta)\frac{\partial \theta}{\partial t} \quad (1)$$

where the viscous function $g(\theta)$ is

$$g(\theta) = \alpha_1 \sin^2\theta \cos^2\theta + \eta_c + (\alpha_2 + \alpha_3)\sin^2\theta \quad (2)$$

Here, the α_i values are Leslie coefficients, and the Miesowicz viscosity $\eta_c = (-\alpha_2 + \alpha_4 + \alpha_5)/2$ is the viscosity when $\theta = 0$. The torque balance for the director in this geometry is

$$\beta\frac{\partial \theta}{\partial t} = (\alpha_3 \sin^2\theta - \alpha_2 \cos^2\theta)\frac{\partial v}{\partial z} + h(\theta)\frac{\partial^2 \theta}{\partial z^2} + \frac{h'(\theta)}{2}\left(\frac{\partial \theta}{\partial z}\right)^2 - \epsilon_a E^2 \sin\theta \cos\theta \quad (3)$$

where $\beta = \alpha_3 - \alpha_2$, which is positive by thermodynamic arguments,[8] $h(\theta) = K_1 \sin^2\theta + K_3 \cos^2\theta$, $h'(\theta)$ is the θ derivative of $h(\theta)$, the anisotropic permittivity ϵ_a is the difference between the permittivity parallel ($\epsilon_\parallel$) and perpendicular ($\epsilon_\perp$) to the director, and E is the strength of the applied electric field. K_1 and K_3 are Frank elastic constants, which are relatively small for liquid crystalline polymer systems.[17,18] Thus, in our treatment, the Frank elasticity terms are neglected, especially since the gradient of the director will also be small for the first several strain units of primary interest in this work.

* Author to whom correspondence should be addressed.
† Present address: Department of Chemical Engineering, Tunghai University, Taichung, Taiwan.

0024-9297/93/2226-1529$04.00/0

Next, we assume that the shear rate, $\dot{\gamma} = \partial v/\partial z$, is a constant, and transform the time variable to strain, $\gamma = \dot{\gamma}t$, so (1) and (3), respectively, become

$$\frac{\tau}{\dot{\gamma}} = \alpha_1 \cos^2\theta \sin^2\theta + \eta_c + (\alpha_2 + \alpha_3)\sin^2\theta + (\alpha_2 \cos^2\theta - \alpha_3 \sin^2\theta)\frac{\partial\theta}{\partial\gamma} \quad (4)$$

and

$$\frac{\partial\theta}{\partial\gamma} = \frac{1}{\beta}(\alpha_3 \sin^2\theta - \alpha_2 \cos^2\theta) - 2\kappa \sin\theta\cos\theta \quad \text{where } \kappa = \frac{\epsilon_a E^2}{2\beta\dot{\gamma}} \quad (5)$$

The parameter κ may be either positive or negative, depending on the sign of ϵ_a, or zero when no electric field is applied. Elimination of $\partial\theta/\partial\gamma$ by substitution of (4) into (5) yields

$$\frac{\tau}{\dot{\gamma}} = \alpha_1 \cos^2\theta \sin^2\theta + \eta_c + (\alpha_2 + \alpha_3)\sin^2\theta - \frac{1}{\beta}(\alpha_2 \cos^2\theta - \alpha_3 \sin^2\theta)^2 - 2\kappa(\alpha_2 \cos^2\theta - \alpha_3 \sin^2\theta)\sin\theta\cos\theta \quad (6)$$

Transient Flow Behavior in the Absence of an Electric Field

If no electric field is maintained during flow, $\kappa = 0$, and (5) and (6), respectively, simplify to

$$\beta\frac{\partial\theta}{\partial\gamma} = \alpha_3 \sin^2\theta - \alpha_2 \cos^2\theta \quad (7)$$

and

$$\frac{\tau}{\dot{\gamma}} = \alpha_1 \cos^2\theta \sin^2\theta + \eta_c + (\alpha_2 + \alpha_3)\sin^2\theta - \frac{1}{\beta}(\alpha_2 \cos^2\theta - \alpha_3 \sin^2\theta)^2 \quad (8)$$

By taking the derivative of τ with respect to θ, it is easily shown from (8) that τ achieves a maximum when $\theta = \pi/4$, as Viola and Baird[5] have noted, subject to the condition that

$$\alpha_1 > -[(\alpha_2 + \alpha_3)^2/(\alpha_3 - \alpha_2)] \quad (9)$$

We now assume that $\alpha_2 < 0$, since no positive value of α_2 has been reported for a liquid crystal. Equation 7 can be integrated using the initial condition that $\theta = 0$ at $\gamma = 0$, for the two separate cases when $\alpha_3 > 0$ (tumbling) and $\alpha_3 < 0$ (flow alignment), to give

$$\gamma = \frac{1 + \delta^2}{\delta}\tan^{-1}(\delta \tan\theta) \quad (10)$$

for the tumbling case and

$$\gamma = \frac{1}{2}\frac{1 - \delta^2}{\delta}\ln\left(\frac{1 + \delta\tan\theta}{1 - \delta\tan\theta}\right) \quad (11)$$

for the flow alignment case, where $\delta = |\alpha_3/\alpha_2|^{0.5}$. Strictly speaking, (11) is valid only when $\delta^2 \tan^2\theta < 1$, but this is always satisfied for an initial orientation of $\theta = 0$ because the steady-state value of $\tan\theta$ is δ^{-1}. Alternately, if an imaginary value of δ is allowed, i.e., $\delta^* = (\alpha_3/\alpha_2)^{0.5}$, the relationship between the orientation angle and strain is given by

$$\gamma = \frac{1 + (\delta^*)^2}{\delta^*}\tan^{-1}(\delta^* \tan\theta) \quad (12)$$

for either real or imaginary δ^*.

In the tumbling case, the stress oscillates[20] with a strain period of

$$\gamma_p = \frac{\pi(1 + \delta^2)}{\delta} \quad (13)$$

The period is independent of the initial orientation of the director.

Since τ is a maximum when $\theta = \pi/4$ for either case, the strain γ_m, at which the maximum shear stress occurs, is given by

$$\gamma_m = \frac{1 + \delta^2}{\delta}\tan^{-1}\delta \quad \text{for the tumbling case} \quad (14)$$

and

$$\gamma_m = \frac{1}{2}\frac{1 - \delta^2}{\delta}\ln\left(\frac{1 + \delta}{1 - \delta}\right) \quad \text{for the flow alignment case} \quad (15)$$

Since δ is less than unity from all experimental reports for liquid crystals, (14) and (15) demonstrate that, for the tumbling case, the maximum shear stress occurs at a strain larger than unity, while it occurs at a strain smaller than unity for the flow alignment case.

In the parellel plate rheometer used in the experimental portion of this work, the normal stress difference $N_1 - N_2$ is measured. $N_1 - N_2$ can be estimated from ELP theory, as shown below. The viscous component of the normal stresses τ_{xx} and τ_{zz} are determined in the 2-D limit as

$$\frac{\tau_{xx}}{\dot{\gamma}} = \alpha_1 \sin^3\theta\cos\theta + \frac{1}{2}(\alpha_5 + \alpha_6)\sin\theta\cos\theta - \frac{1}{2}(\alpha_2 + \alpha_3)\sin\theta\cos\theta + (\alpha_2 + \alpha_3)\sin\theta\cos\theta\frac{\partial\theta}{\partial\gamma} \quad (16)$$

and

$$\frac{\tau_{zz}}{\dot{\gamma}} = \alpha_1 \sin\theta\cos^3\theta + \frac{1}{2}(\alpha_5 + \alpha_6)\sin\theta\cos\theta + \frac{1}{2}(\alpha_2 + \alpha_3)\sin\theta\cos\theta - (\alpha_2 + \alpha_3)\sin\theta\cos\theta\frac{\partial\theta}{\partial\gamma} \quad (17)$$

Since τ_{yy} is presumed to be zero in the 2-D treatment, the normal stress difference $N_1 - N_2 = \tau_{xx} - 2\tau_{zz}$ in our coordinate system, so

$$\frac{N_1 - N_2}{\dot{\gamma}} = \alpha_1(\sin^3\theta\cos\theta - 2\sin\theta\cos^3\theta) - \frac{1}{2}(\alpha_5 + \alpha_6)\sin\theta\cos\theta - \frac{3}{2}(\alpha_2 + \alpha_3)\sin\theta\cos\theta + 3(\alpha_2 + \alpha_3)\sin\theta\cos\theta\frac{\partial\theta}{\partial\gamma} \quad (18)$$

Transient Startup with Concurrent Electric Field

For the case where an electric field is applied during shear startup, i.e., when κ is nonzero, setting to zero the derivative of (4) with respect to θ gives

$$0 = \sin 2\theta\{(\alpha_1 + (\alpha_2 + \alpha_3)^2/\beta)\cos 2\theta - \kappa[(\alpha_2 - \alpha_3)\cot 2\theta + (\alpha_2 + \alpha_3)\cos 2\theta \cot 2\theta - (\alpha_2 + \alpha_3)\sin 2\theta]\} \quad (19)$$

For the case of small κ to be considered in the following perturbation analysis, we expect the angle θ_m, where the shear stress maximum occurs, to be near the zero-field value of $\pi/4$, so we can divide (19) through by $\sin 2\theta$. Next, we expand θ_m in a power series about κ as

$$\theta_m = \theta_{m0} + \kappa\theta_{m1} + O(\kappa^2) \quad (20)$$

Substitution of (20) into (19) yields

$$\theta_m = \pi/4 + \kappa\frac{1}{2}\frac{\beta(\alpha_2 + \alpha_3)}{\alpha_1\beta + (\alpha_2 + \alpha_3)^2} + O(\kappa^2) \quad (21)$$

For an LCP of positive dielectric anisotropy, the angle θ_m is less than $\pi/4$ because the numerator of the κ term in

(21) is negative whenever $\delta < 1$ (for negative α_2), while the denominator is positive as a result of the inequality in (9).

The strain γ_m, at which θ_m occurs when an electric field is applied, can also be found by expanding θ and γ_m in powers of κ and integrating the resulting perturbation approximations from (5). For the tumbling case where $\alpha_2\alpha_3 < 0$, the result is

$$\gamma_m = \frac{1+\delta^2}{\delta}\tan^{-1}\delta + \kappa(1+\delta^2)\left(1 - \frac{1-\delta^2}{(1-\delta^2)^2 - (1+\delta^2)\alpha_1/\alpha_2}\right) \quad (22)$$

Details of the calculation are given in Appendix A. For a material of positive dielectric anisotropy, imposition of the electric field causes the strain at maximum stress to shift to lower values of strain provided α_1 satisfies the inequality

$$\delta^2\frac{1-\delta^2}{1+\delta^2}|\alpha_2| > \alpha_1 > \frac{(1-\delta^2)}{1+\delta^2}\alpha_2 \quad (23)$$

Carlsson and Skarp have demonstrated that application of a sufficiently strong transverse electric field to a tumbling nematic undergoing shear will suppress the occurrence of tumbling and cause the director to assume a flow aligned angle.[19,21] In our nomenclature, this will occur when a critical value of κ is reached, namely

$$\kappa_c = (-\alpha_2\alpha_3)^{1/2}/\beta \quad (24)$$

At this critical field, γ_m is given by

$$\gamma_m = 1 + \delta[\phi/(1+\phi)] \quad (25)$$

where $\phi = \alpha_1/|\alpha_2|$. The derivation for this expression is given in Appendix B and was arrived at by a perturbation expansion in δ, rather than in κ as before, because κ_c is not necessarily less than unity. Because δ is normally quite small, γ_m at the critical field is usually near unity.

Experimental Section

The poly(*n*-hexyl isocyanate) (PHIC) used in the rheological studies described here was synthesized in our laboratory by anionic polymerization, following the procedure of Shashoua.[22] The polymer had a viscosity average molecular weight of 180 000, while the polydispersity, $\overline{M_w}/\overline{M_n}$, was about 2.3 by GPC. Solutions of the synthesized polymer in *p*-xylene were found to be biphasic between 20 and 24 wt %. The concentration studied was 26 wt % (23.3 vol %), which was fully liquid crystalline by microscopic observation in the quiescent state.

A 60-Hz ac electric field (1.5–2.0 MV/m, rms) was applied to flat electrodes to orient the PHIC molecules perpendicular to the electrode surfaces (homeotropic orientation). Formation of a unidomain under these conditions was verified by both polarized light microscopy and conoscopy. Approximately 10 min of electrical orientation was required to establish the unidomain. The time scale for destruction of the unidomain after removal of the electric field was also several minutes, as determined by observing the rate of decay of the conoscopic interference figure. In our transient experiments, only strains less than seven are analyzed, corresponding to less than 20 s following removal of the electric field, so degradation of the orientation due to sources other than the flow field is not likely to be significant.

Rheological measurements were performed in a Rheometrics RMS800 rotational rheometer using either cone and plate or insulated parallel plate fixtures, across which the orienting electric field was applied. All measurements on unidomain samples were done using the parallel plate geometry, because of the need to provide a uniform electric field. Unfortunately, the parallel plate geometry does not provide a uniform shear field, because the shear rate varies linearly with radial position. However, steady-state viscosity measurements on polydomain samples using the cone and plate geometry agreed well with those using a parallel plate geometry, when the latter were determined using the Rabinowitsch correction.[23] A comparison of transient test runs on polydomain samples using cone and plate and parallel plate fixtures showed that the same characteristics of the shear stress response were observed in both geometries.

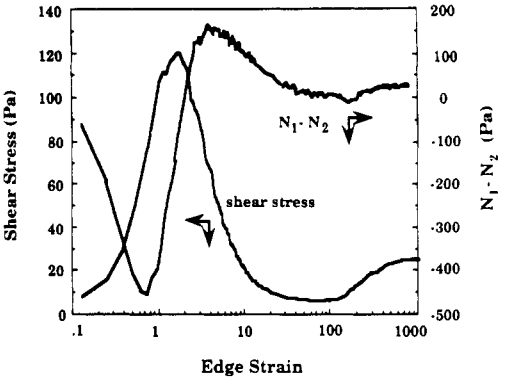

Figure 2. Transient shear and normal stresses for unidomain PHIC solution. Edge shear rate is 0.4 s^{-1}.

A unidomain texture was created in the rheometer by applying an ac field for at least 30 min to a quiescent sample. Following electrical orientation, shear flow was suddenly initiated, with either simultaneous elimination of the electric field or else simultaneous change of value of the electric field. Transient shear flow for the nonoriented, polydomain sample was initiated following 30 min of sample relaxation after the solution was loaded in the rheometer; longer initial relaxation times did not affect the transient polydomain response. Torque and normal force were monitored as a function of time, though the latter values were reliable only for the electrically oriented unidomain samples. Further details of the experimental procedures are available elsewhere.[23,24]

Results

The steady-state viscosity[23] of the PHIC solution exhibited a constant plateau region between shear rates of 0.1 and 1.0 s^{-1}. A shear thinning region started at about 1.0 s^{-1}; the slope of a plot of log η vs log $\dot{\gamma}$ in this region was −0.6, which is very close to that reported for other liquid crystalline polymer systems.[1,25]

Figure 2 shows the transient shear stress and transient normal stress difference $N_1 - N_2$ of a unidomain PHIC solution at an edge shear rate of 0.4 s^{-1}. In this case, the electric orienting field was removed when the shear flow was started. Both the shear stress and normal stress are reported as apparent values since the Rabinowitsch correction could not be applied. The shear stress exhibited a single large overshoot followed by a broad undershoot before reaching steady state. The normal stress difference $N_1 - N_2$ showed an initial large negative undershoot, followed by a positive overshoot and a monotonic decrease to reach a positive steady-state value. The negative undershoot of $N_1 - N_2$ occurred at a smaller strain than did the overshoot of the shear stress. Similar behaviors were found at other shear rates studied, ranging from 0.4 to 10 s^{-1}.

The shear stress response of unidomain PHIC at different shear rates is shown in Figure 3. At the lower shear rates, 0.4–1.0 s^{-1}, the normalized shear stress response scaled with strain. The stress exhibited a large overshoot of about 5 times the steady value, followed by an undershoot and a gradual approach to steady state. The overshoot appeared at an edge strain of about 1.6, while the undershoot was very broad, requiring about 700 strain units to reach steady state. At higher shear rates, in the shear thinning region, the normalized shear stress also scaled with strain, but followed a different master curve.

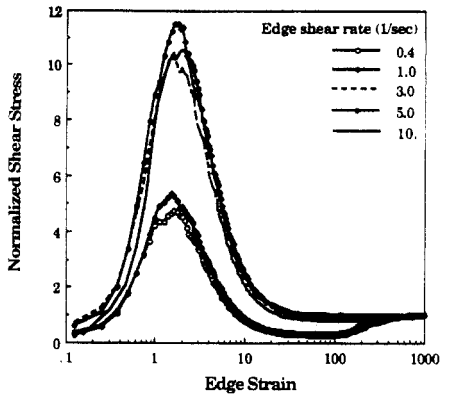

Figure 3. Response of a unidomain PHIC solution to sudden shear startup.

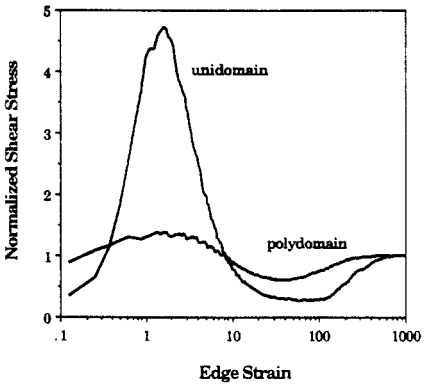

Figure 4. Transient shear stress response of unidomain and polydomain PHIC solutions. Both sets of data were acquired in a parallel plate geometry at an edge shear rate of 0.4 s^{-1}.

At higher shear rates the overshoot occurred at about the same strain as those at low shear rates, but the magnitude of the overshoot was even larger, about 11 times the steady value. No appreciable undershoot was observed at the higher shear rates, and steady state was reached within 100 strain units.

The transient results of shear startup for both unidomain and polydomain solutions are compared in Figure 4. Both show a similar oscillatory stress response. The overshoots for both unidomain and polydomain samples occurred at essentially the same time (or strain), but the magnitude in the polydomain case was greatly reduced. Similarly, the minima of the undershoots occurred at nearly the same strain, but the undershoot for the oriented sample was deeper and broader than that of the polydomain sample. As expected, both samples had the same steady-state viscosity, since it reflected the solution structure at steady state. Thus, both unidomain and polydomain solutions showed the same response to the startup of shear flow, except for a difference in amplitude. The same relative behavior of unidomain vs polydomain samples was found at all of the shear rates studied.

When a unidomain sample was sheared with a dc electric field maintained during shear flow, the steady-state shear stress increased with increasing applied field strength. However, the amplitude of the stress oscillation was suppressed, while the magnitude of the strain at which the overshoot peak occurred also decreased, as can be seen in Figure 5. With increasing field strength, the peak shifted from its zero-field value of 1.6 to smaller strain, while the undershoot became shallower and narrower. At fields greater than 0.375 MV/m, the peak occurred at an edge strain less than unity, while the undershoot also disappeared. With further increases of the field strength, the magnitude of the stress overshoot became smaller.

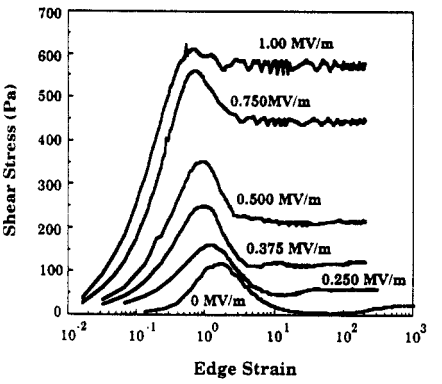

Figure 5. Stress response of unidomain PHIC solution to sudden shear startup with simultaneous application of dc electric field.

Discussion

The shear stress response of a unidomain PHIC nematic to sudden shear startup indeed scales with strain, as ELP theory predicts, and has been observed for other polydomain LCPs. However, two separate master curves are seen for unidomain PHIC: one for shear rates in the constant-viscosity plateau (region II, according to Onogi and Asada[26]) and one for shear rates in the shear thinning region (region III). Since linear ELP theory cannot describe such nonlinear behavior as a shear thinning steady-state viscosity, it is not surprising that transient behavior in this nonlinear regime is different from that in the lower shear rate regime in which ELP theory is expected to be valid.

Quantitative information (e.g., the sign and magnitude of α_3) cannot be extracted directly via the previous analysis from the data in Figure 2, because the measurements were not performed at a uniform shear rate. For example, when the sample in a parallel plate apparatus experiences an edge strain of unity, all of the material except that at the edge has actually experienced a strain less than unity. Hence, in the parallel plate geometry, location of the stress maximum at an edge strain somewhat larger than unity will serve as the demarcation between tumbling and nontumbling behavior.

By assuming that an LCP sample in the parallel plate geometry consists of concentric cylinders of material which are rheologically independent of each other, we have applied the 2-D ELP treatment given previously to the layers, each of which has its individual value of uniform strain. We have numerically summed the contributions to the stress from each layer and have determined the location of the stress maximum, which is a unique function of $\alpha_3/|\alpha_2|$. In the absence of an electric field, the edge strain γ_{mR} at which the shear stress maximum occurs in the parallel plate mode is approximately 0.25 strain unit larger than γ_m as calculated from either (14) or (15). This difference of +0.25 strain unit agrees well with the value of +0.2 found via a perturbation expansion for a material having a constant steady-state viscosity and a transient stress behavior that is only a function of strain.[24] A plot of γ_{mR} vs δ^2 is presented in Figure 6. The maximum in the observed experimental shear stress at 0.4 s^{-1} always occurred at an edge strain greater than 1.25.

In a homogeneous shear flow such as that generated in a cone and plate rheometer, periodic undamped stress oscillations are predicted by ELP theory.[20] However, in a parallel plate geometry, these stress oscillations are damped as a result of destructive interference due to the phase differences between the material at different radial positions. Ultimately, the stress reaches a steady-state value which is the average of a single undamped cycle.[24]

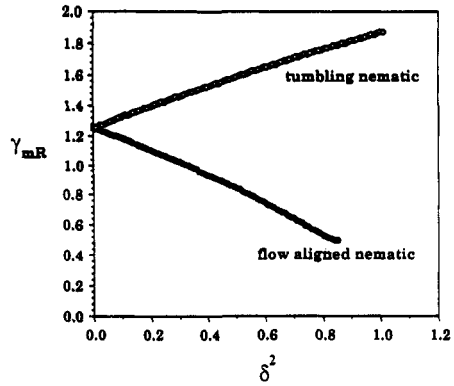

Figure 6. Edge strain location of the transient shear stress maximum. $\delta^2 = |\alpha_3/\alpha_2|$.

Thus, the characteristics of the transient stress response of a unidomain PHIC solution at 0.4 s^{-1} are consistent with those of a tumbling nematic—a damped stress oscillation and a stress maximum occuring at an edge strain greater than 1.25. Although it is possible, in principle, to determine $\alpha_3/|\alpha_2|$ from the strain at the highest stress measured, in practice this is difficult to do because of the inherent experimental noise in the rheometric stress signal. For example, in nine repeat experiments at 0.4 s^{-1}, the highest value of stress measured occurred at an average edge strain of 1.62, with a standard deviation of 0.17, while stress levels within 5% of the maximum were recorded over an edge strain range of 1.2–2.2.

Because of this variability, we elected to identify the experimental values of the Leslie coefficients by numerically curve fitting the combined stress data from multiple experimental runs to the 2-D version of ELP theory that has been modified to account for the radial variation in shear rate. A total of four independent parameters, α_1, α_2, α_3, and η_c, define the shape of the stress vs. strain curve. A fifth parameter, the Miesowicz viscosity η_b when the director is aligned parallel to the flow direction, can be calculated from the relation $\eta_b = \eta_c + \alpha_2 + \alpha_3$. A Runge–Kutta technique was used to generate theoretical predictions, while a least-squares simplex method was used to determine the best fit parameters. Data points were equally weighted from the strain range 0.5–7.0. A strain of 0.5 was chosen as a lower limit because the assumption of constant strain rate is not valid at low strain, as (8) predicts that the stress is nonzero at $\gamma = 0$. A strain of 7 was chosen as the upper limit, since inclusion of points beyond a strain of 7 produced best fit parameters that differed markedly from those found when the upper strain limit ranged from 3 to 7.

Figure 7 shows experimental data points together with the predicted values using the best fit parameters shown in Table I. The values of the best fit parameters are consistent with the inequalities in (9) and (23) and $\delta < 1$, so the curve fit parameters satisfy all restrictions in the 2-D theory. Uncertainties in the parameters were estimated by a sensitivity analysis which held three parameters fixed while varying the fourth in such a fashion as to ensure that >95% of the experimental data points fell between the curves predicted using the upper and lower uncertainty bounds for the given parameter. For comparison in Table I, we have also listed values estimated from the steady-state electroviscosity measurements[23] and predictions from Kuzuu and Doi[27] for our PHIC solution. Compared to the current analysis based on transient behavior, the governing equations for the steady-state electroviscosity are relatively insensitive to α_1, α_2, and α_3, so we believe the present estimates for these coefficients are more reliable. The

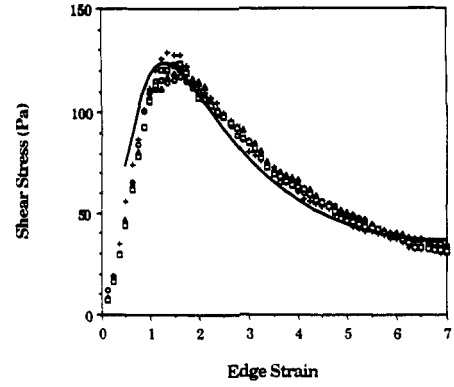

Figure 7. Comparison of experimental shear stress transients with ELP theory for PHIC solution at edge strain of 0.4 s^{-1}. (○, +, ▲, □) Experimental; (—) prediction using best fit parameters from Table I.

Table I
Estimates of Leslie Coefficients for PHIC Solution

parameter	this work	electroviscosity[23]	Kuzuu and Doi[27]
α_1 (Pa s)	−910 ± 160[a]	−1100	−2590
α_2	−2490 ± 80	−3700	−3770
α_3	230 ± 80	320	169
α_4			159
α_5			3310
α_6			−290
η_c	2360 ± 70	2100	3640
η_b	100 ± 230	(−1280)[b]	39
E_c (MV/m)	0.34	0.4	0.35

[a] Uncertainty estimated over strain range 0.5–6.5. [b] Negative value not physically realistic.

absolute values of the parameters predicted by Kuzuu and Doi tend to be somewhat larger than our estimates from the experimental data. Of course, our PHIC molecules were neither perfectly rigid nor monodisperse, as Doi theory presumes, and it is unlikely that the initial orientation distribution induced by the electric field in our experiments corresponds to the equilibrium distribution assumed in Kuzuu and Doi's calculation of the Leslie parameters.

Using the best fit Leslie parameters from the transient shear stress, we have predicted the transient normal stress response for the parallel plate geometry used. The normal stress difference $N_1 - N_2$ was measured in the parallel plate geometry. As can be seen from (18), two additional Leslie coefficients, α_5 and α_6, are needed to describe the normal stress behavior. Since the Parodi relation gives $\alpha_2 + \alpha_3 = \alpha_6 - \alpha_5$, only one of these is independent. We have chosen values for α_5 and α_6 such that the ratio α_5/α_6 is the same as that predicted by Kuzuu and Doi, but other reasonable estimates for α_5 and α_6 gave similar predictive curves. As Figure 8 demonstrates, the predicted curves faithfully reproduce the features of the observed behavior at small strain, confirming the reliability of the parameter values. At larger strain, damped oscillations are predicted by the theory but not observed experimentally.

Use of the 2-D approximation to describe our experimental results warrants some discussion, since out-of-plane deviations of the director are known to occur for tumbling liquid crystals[28] and LCPs.[29] However, these 3-D deviations have been observed for tumbling nematics which are initially oriented near the flow direction. A stability analysis by Zuniga and Leslie[30] suggests that a nematic which has an initial homeotropic orientation (as in our experiments) will only become unstable to perturbations out of the shearing plane if the orientation at the center of the gap has crossed the flow direction, i.e., for $\theta > \pi/2$ in our nomenclature. Since the curve fitting analysis of

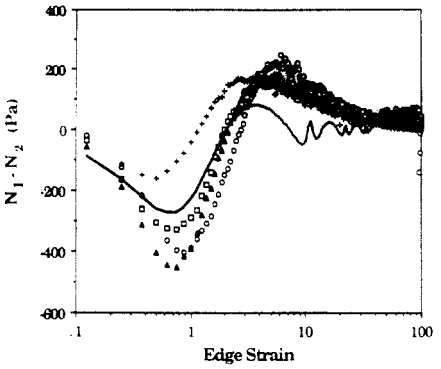

Figure 8. Comparison of experimental normal stress transients with ELP theory for PHIC solution at edge strain of 0.4 s^{-1}. (○, +, ▲, □) Experimental; (—) prediction using α_1, α_2, and α_3 from Table I and α_5 = 2080 Pa s, α_6 = −180 Pa s.

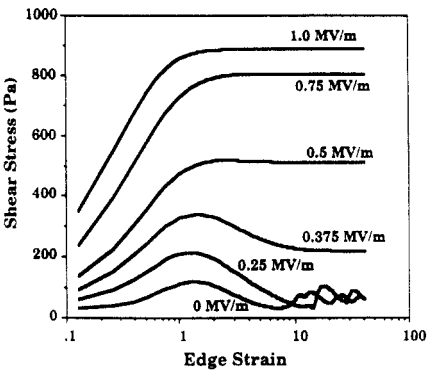

Figure 9. Predicted transient response of PHIC solution to sudden shear startup at edge shear rate of 0.4 s^{-1} with concurrent application of dc electric field.

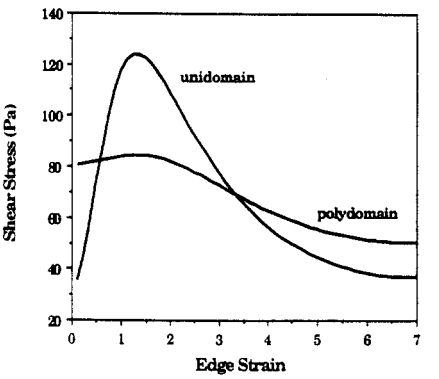

Figure 10. Predicted shear stress response of polydomain nematic in parallel plate geometry for sudden shear startup. The initial orientation distribution of domains was assumed to be random.

our experimental transient data at small strains only involves $\theta < \pi/2$, it is reasonable to assume that 3-D instabilities do not occur in this case. However, such instabilities may occur at higher strains when θ exceeds 90°, perhaps accounting for the lack of observed oscillations in the shear and normal stress, despite a prediction of oscillations by the 2-D theory. Rheooptical measurements during shear startup of an initially homeotropic LCP could provide definitive information on the occurrence of any 3-D instabilities.

Theoretical predictions of the transient response to sudden shear startup have been made by Marrucci and Maffettone[31] on the basis of a 2-D approximation of Doi theory. For an initial condition of uniform orientation parallel to the velocity gradient, their work in the tumbling regime predicts an initial negative undershoot for normal stress and that the undershoot occurs at smaller strain than does the overshoot of the shear stress. Their theoretical predictions are qualitatively consistent with our experimental measurements, but we have not made a quantitative comparison since we do not have estimates for the needed parameters for PHIC.

The transient response of unidomain PHIC when an electric field is maintained during shear startup is seen from Figure 5 to follow qualitatively the predictions from 2-D ELP theory for a nematic with $\alpha_3 > 0$. Specifically, the location of the stress maximum decreases with increasing electric field strength, and the undershoot disappears above a critical value of the applied field where tumbling is suppressed. Because the PHIC solution is not a linear dielectric, ϵ_a is not constant, but is a function of field strength, ranging from 530 to 630 times the permittivity of free space over the range of electric field strength used experimentally. Using this field-dependent value for ϵ_a, together with the Leslie coefficients estimated from the transient shear stress in the absence of an applied field, we show predictions for the transient response with a concurrent field in Figure 9. Quantitative agreement between predictions and experiments is not so good as that seen for the normal stress difference. The critical field strength for the suppression of tumbling is estimated at E_c = 0.34 MV/m from the Leslie coefficients, which agrees well with the field of 0.375 MV/m required to suppress the stress undershoot. The edge strain at which the stress maximum occurs at the critical field is predicted to be 1.30 and observed experimentally to be 1.00 at a field of 0.375 MV/m. The calculations also predict a suppression of the overshoot at a much lower field than is observed experimentally.

Our experimental observations clearly demonstrate that the unidomain and polydomain LCPs respond in the same fashion to a sudden shear startup, with the magnitude of the response diminished in the polydomain case. Analogous to Marrucci and Maffettone,[31] we assume as a simple model that the polydomain structure can be regarded as an ensemble of domains, with each domain having a uniform director and the same Leslie coefficients as the unidomain. If the initial orientation distribution of domains is assumed to be random in 2-D space and if interactions across domain boundaries are neglected, then ELP theory can predict a response for a polydomain sample. A comparison of predicted transient shear stress for the unidomain and polydomain cases is shown in Figure 10; corresponding experimental data are shown in Figure 4. A diminished amplitude of the stress oscillation is seen in the polydomain case, although the extrema occur at the same strain as in the unidomain case. Domains which are initially oriented at $\theta = \pi/2$ maintain an orientation near this angle for a relatively long time, since the torque experienced at this angle is quite small. Rather, domains with initial orientation near $\theta = 0$ will dominate the initial transient stress response. Our results could be interpreted as evidence that domain boundaries are relatively unimportant in initial shear transient behavior, which could explain the ability of unidomain theories to describe the qualitative transient behavior of polydomain samples.[5] Since the period of oscillation is independent of the initial orientation, it may be possible to estimate α_3/α_2 from the stress oscillations of a polydomain sample.

Although the 2-D ELP theory agrees quantitatively with our transient experiments at small strains (<7), it clearly fails to describe the behavior even qualitatively at much larger strains, including steady state. Most notably, the multiple stress oscillations predicted by ELP theory for a tumbling nematic are never observed in our PHIC system.

This may be due to a breakdown in the two-dimensional hypothesis or some unaccounted-for interactions, such as domain boundaries, Frank elasticity, or degradation of the electrically imposed unidomain. We note that not all LCPs show multiple stress oscillations experimentally, and at least one LCP, poly(benzobisthiazole), has even been found to exhibit either persistent oscillations or else a single overshoot with a weak undershoot, depending on the solvent used to form the lyotropic solution.[32]

Conclusions

We have presented experimental measurements of the shear startup for a unidomain liquid crystalline polymer and found that the initial transient behavior is quantitatively well-described by the theory of Ericksen, Leslie, and Parodi. Thus, rheological transient behavior can be used to estimate the Leslie coefficients for a unidomain; specifically, the strain at which the shear stress maximum occurs provides information on the sign of α_3. A solution of 26 wt % PHIC in *p*-xylene was found to have a positive α_3 at a shear rate in the constant viscosity region II plateau. Unidomain and polydomain solutions showed qualitatively similar behavior, so it may be possible to estimate unidomain parameters from the more easily obtained polydomain data. Application of a transverse electric field during shear startup causes both the magnitude and strain location of the stress maximum to decrease for a tumbling LCP with positive dielectric anisotropy, such as PHIC, because the orientation angle at maximum stress occurs nearer to the initial orientation.

Acknowledgment. The support of the National Science Foundation for this work under Research Initiation Grant MSS-8996205 was greatly appreciated. We are also grateful to the reviewers for insightful suggestions.

Appendix A. Location of γ_m for a Tumbling LCP in an Electric Field

To solve for γ_m, the relation of strain to the orientation of the director must be solved from eq 5, so we expand θ in powers of κ, i.e., $\theta = \theta_0 + \kappa\,\theta_1 + O(\kappa^2)$. Substituting (20) into (5) and collecting like-order terms give

$$\frac{\partial\theta_1}{\partial\gamma} = \left[\frac{\theta_1}{\beta}(\alpha_3 + \alpha_2) - 1\right] \sin 2\theta_0 \qquad \text{(A1)}$$

subject to the initial condition at $\gamma = 0$, $\theta_1 = 0$. For the zero-field tumbling case, γ is given by (10) with $\theta = \theta_0$, while integration of (A1) yields

$$\theta_1 = \beta \sin^2 \theta_0/\alpha_2 \qquad \text{(A2)}$$

Thus

$$\theta = \theta_0 + \kappa\beta \sin^2 \theta_0/\alpha_2 + O(\kappa^2) \qquad \text{(A3)}$$

For a material of positive dielectric anisotropy, θ is always less than θ_0, because α_2 is negative. Thus, for a given value of strain, the orientation angle achieved with a field applied is less than the value it would achieve if no field were applied. Physically, this occurs because the electric field induces the molecules to orient toward $\theta = 0$; of course, for a material with negative dielectric anisotropy, the field induces orientation toward $\theta = \pi/2$, and the orientation angle would be greater than that without a field, as (A3) indicates.

At γ_m, $\theta = \theta_m$, so (21) is equal to (A3), and

$$\theta_m = \frac{\pi}{4} + \frac{\kappa\beta(\alpha_2 + \alpha_3)}{2[\alpha_1\beta + (\alpha_2 + \alpha_3)^2]} = \theta_0 + \frac{\kappa\beta}{\alpha_2}\sin^2\theta_0 \qquad \text{(A4)}$$

θ_0 in this expression is the orientation angle of the director which would occur in the absence of an electric field *at the same strain* where the stress maximum occurs in the presence of the electric field.

Taking the tangent of both sides in (A4) and retaining only first-order terms in κ give

$$\tan\frac{\pi}{4} + \kappa\frac{\beta(\alpha_2 + \alpha_3)}{\alpha_1\beta + (\alpha_2 + \alpha_3)^2} = \tan\theta_0 + \kappa\frac{\beta}{\alpha_2}\tan^2\theta_0 \qquad \text{(A5)}$$

From (10)

$$\tan\theta_0 = \frac{1}{\delta}\tan\frac{\delta\gamma_m}{1 + \delta^2} \qquad \text{(A6)}$$

Next, we expand γ_m about κ as $\gamma_m = \gamma_{m0} + \kappa\gamma_{m1}$, where γ_{m0} is the strain at which the stress maximum would occur in the absence of a field. Substituting this expansion into (A6) and retaining first-order terms in κ yield

$$\tan\theta_0 = \frac{1}{\delta}\tan\left(\frac{\delta\gamma_{m0}}{1 + \delta^2}\right) + \frac{\kappa\gamma_{m1}}{1 + \delta^2}\sec^2\left(\frac{\delta\gamma_{m0}}{1 + \delta^2}\right) \qquad \text{(A7)}$$

Since $\gamma_{m0} = [(1 + \delta^2)/\delta]\tan^{-1}\delta$ from (14), the zero-order term in (A7) is unity and $\sec^2(\delta\gamma_{m0}/(1 + \delta^2)) = 1 + \delta^2$, so

$$\gamma_{m1} = (1 + \delta^2)\left[1 - \frac{1 - \delta^2}{(1 - \delta^2)^2 - (1 + \delta^2)\alpha_1/\alpha_2}\right] \qquad \text{(A8)}$$

and γ_m is then given by (22).

Appendix B. Location of Maximum Shear Stress at Critical Field Strength for Tumbling Nematics

At the critical field strength, $\kappa = |\alpha_2\alpha_3|^{0.5}/\beta$, so (5) becomes

$$\frac{\partial\theta}{\partial\gamma} = \frac{1}{\beta}(\alpha_3^{1/2}\sin\theta - |\alpha_2|^{1/2}\cos\theta)^2 \qquad \text{(B1)}$$

Dividing both sides by $\cos^2\theta$ and integrating from the initial condition of $\gamma = 0$ at $\theta = 0$ yield

$$\tan\theta = \gamma/(1 + \delta^2 + \delta\gamma) \qquad \text{(B2)}$$

Substitution of (B1) into (4), differentiation with respect to θ, and elimination of sin 2θ as before give

$$0 = \left(\frac{\alpha_1}{|\alpha_2|} + \frac{(1 - \delta^2)^2}{1 + \delta^2}\right)\cos 2\theta - \frac{\delta}{1 + \delta^2}(1 - \delta^2)\sin 2\theta + \delta\cot 2\theta + \frac{\delta(1 - \delta^2)}{1 + \delta^2}\cos 2\theta\cot 2\theta \qquad \text{(B3)}$$

We expand θ_m in terms of δ as $\theta_m = \theta_{m0} + \delta\theta_{m1} + O(\delta^2)$, substitute this into (B3), and collect the zero- and first-order terms. Since $\cos 2\theta_{m0} = 0$, then $\theta_{m0} = \pi/4$ and sin $2\theta_{m0} = 1$ and cot $2\theta_{m0} = 0$. Collection of the first-order terms gives

$$\theta_{m1} = -\frac{1}{2}\left(\frac{\alpha_1}{|\alpha_2|} + 1\right)^{-1} \qquad \text{(B4)}$$

Thus, $\theta_m = \pi/4 - \delta/2(1 + \phi) + O(\delta^2)$, where $\phi = \alpha_1/|\alpha_2|$.

By expanding $\gamma_m = \gamma_{m0} + \delta\gamma_{m1} + O(\delta^2)$ and substituting θ_m into (B2), we arrive at

$$1 - \delta\frac{1}{1 + \phi} + O(\delta^2) = \gamma_{m0} + \delta(\gamma_{m1} - \gamma_{m0}) + O(\delta^2) \qquad \text{(B5)}$$

So $\gamma_{m0} = 1$ and $\gamma_{m1} = \phi/(1 + \phi)$, or $\gamma_m = 1 - \delta\phi/(1 + \phi)$, which is (25).

References and Notes

(1) Kiss, G.; Porter, R. S. *J. Polym. Sci., Polym. Phys. Ed.* **1980**, *18*, 361.
(2) Grizzuti, N.; Cavella, S.; Cicarelli, P. *J. Rheol.* **1990**, *34*, 1293.
(3) Gotsis, A. D.; Baird, D. G. *Rheol. Acta* **1986**, *25*, 2275.

(4) Moldenaers, P.; Mewis, J. *J. Rheol.* **1986**, *30*, 568.
(5) Viola, G. G.; Baird, D. G. *J. Rheol.* **1986**, *30*, 601.
(6) Picken, S. J.; Aerts, J.; Doppert, H. L.; Reuvers, A. J.; Northolt, M. G. *Macromolecules* **1991**, *24*, 1366.
(7) Ericksen, J. L. *Arch. Ration. Mech. Anal.* **1960**, *4*, 231.
(8) Leslie, F. M. *Q. J. Mech. Appl. Math.* **1966**, *19*, 357.
(9) Parodi, O. *J. Phys. (Paris)* **1970**, *31*, 581.
(10) Hess, S., *Z. Naturforsch.* **1976**, *31A*, 1034.
(11) Hess, S., *Z. Naturforsch.* **1976**, *31A*, 1507.
(12) Doi, M. *J. Polym. Sci., Polym. Phys. Ed.* **1981**, *19*, 229.
(13) Marrucci, G.; Maffettone, P. L. *Macromolecules* **1989**, *22*, 4076.
(14) Marrucci, G. *Macromolecules* **1991**, *24*, 4176.
(15) Berry, G. C. *J. Rheol.* **1991**, *35*, 943.
(16) Burghardt, W. R.; Fuller, G. G. *Macromolecules* **1991**, *24*, 2546.
(17) Taratuta, V. G.; Hurd, A. J.; Meyer, R. B. *Phys. Rev. Lett.* **1985**, *55*, 246.
(18) Se, K.; Berry, G. C. *Mol. Cryst. Liq. Cryst.* **1987**, *153*, 133.
(19) Carlsson, T.; Skarp, K. *Mol. Cryst. Liq. Cryst.* **1981**, *78*, 157.
(20) Marrucci, G. *Pure Appl. Chem.* **1985**, *57*, 1545.
(21) Skarp, T.; Carlsson, T.; Lagerwall, S. T.; Stebler, B. *Mol. Cryst. Liq. Cryst.* **1981**, *66*, 199.
(22) Shashoua, V. E.; Sweeny, W.; Tietz, F. R. *J. Am. Chem. Soc.* **1960**, *82*, 866.
(23) Yang, I-K.; Shine, A. D. *J. Rheol.* **1992**, *36*, 1079.
(24) Yang, I-K. The Rheology of an Electrically Oriented Liquid Crystalline Polymer. Ph.D. dissertation, University of Delaware, 1992.
(25) Einaga, Y.; Berry, G. C.; Chu, S. G. *Polym. J.* **1985**, *17*, 239.
(26) Onogi, S.; Asada, T. In *Rheology*; Astarita, G.; Nicolais, N., Eds.; Plenum Press: New York, 1980; p 127.
(27) Kuzuu, N.; Doi, M. *J. Phys. Soc. Jpn.* **1984**, *53*, 1031.
(28) Pieranski, P.; Guyon, E. *Phys. Rev. A* **1974**, *9*, 404.
(29) Scrinvasarao, M.; Berry, G. C. *J. Rheol.* **1991**, *35*, 379.
(30) Zuniga, I.; Leslie, F. M. *Europhys. Lett.* **1989**, *9*, 689.
(31) Marrucci, G.; Maffettone, P. L. *J. Rheol.* **1990**, *34*, 1217.
(32) Chow, A. W.; Hamlin, R. D.; Ylitalo, C. M. *Macromolecules* **1992**, *25*, 7135.

Registry No. Supplied by Author: PHIC, 26746-07-6.